

## Effects of Different Boundary Conditions at the Surfaces of the Extended Computational Domain in Computing the Natural Convection Flow in an Open Cavity

Roushanara Begum<sup>1</sup> and M. Z. I. Bangalee<sup>2,\*</sup>

<sup>1</sup>Department of Mathematics, Dhaka University, Dhaka 1000, Bangladesh

<sup>2</sup>Department of Applied Mathematics, Dhaka University, Dhaka 1000, Bangladesh

(Received: 18 May 2015; Accepted: 29 Nov 2015)

### Abstract

Effects of different boundary conditions at the surfaces of the extended computational domain on buoyancy driven natural convection flow in a three dimensional open cavity are studied numerically. This study is carried out for turbulent flow where Rayleigh number is greater than  $10^8$ . Air is used as working fluid having properties at 25°C temperature and 1atm pressure. To capture the turbulent nature of the flow  $k - \varepsilon$  model is used. ANSYS CFX software is used to solve the governing equations subject to the corresponding boundary conditions. The methodology is verified through a satisfactory comparison with some published results. Average mass flow, temperature, stream line, contour velocity and velocity profile are studied at different height. An extended computational domain around the physical domain of the cavity at different surrounding conditions is considered to investigate the effect of its existence on the computation. Effects of different surrounding boundary conditions on the physical domain of the cavity are studied and reported. A relation among non-dimensional parameters such as Nusselt number, Rayleigh number, Prandtl number and Reynolds number is also reported.

**Keywords:** Computational fluid dynamics (CFD), Buoyancy,  $k - \varepsilon$  turbulence model, Mass flow rate

### I. Introduction

Natural convection is a mechanism, in which the fluid motion is not generated by any external source but only by density differences in the fluid occurring due to temperature gradients. Buoyancy driven natural convection heat transfer is one of the dominant concepts with many usages in different fields of science and industry. In different applications we need more or less to know about this phenomenon to control it and should be aware how to control it in some cases. Setting the proper boundary conditions is a challenging task due to the complexity of the physical mechanisms involved.

Significant differences may be found in the flow and heat flux profiles in natural convection with Boussinesq assumption and with temperature dependent physical properties, namely density, dynamic viscosity, thermal conductivity and specific heat capacity<sup>1</sup>. If imposing the boundary conditions at the openings of the original model is avoided<sup>2</sup>, the ventilation rate ( $Q$ ) becomes maximum at  $\theta = 45^\circ$  and minimum at  $\theta = 67.5^\circ$ . Relation between the flow rate and the power becomes  $Q = 0.0035(\dot{q})^{0.31}$ . Relation between non-dimensional parameters becomes  $Nu = 0.189Pr^{0.5}Re^{0.8}$  and  $Nu = 0.69Pr^{0.2}Ra^{0.2}$ .

The natural convection flow consists of a horizontal counter flow that penetrates a horizontal cavity over a distinct length, is proportional to the cavity height and the square root of the Rayleigh number<sup>3</sup>. Fusegi et al.<sup>4,5</sup> presented three-dimensional calculations for laminar flow for  $Ra_{up}$  to  $10^{10}$ . Comparisons were made with two-dimensional simulations and differences were reported for the heat transfer correlation between  $Nu$  and  $Ra$ .

An accurate set of effective boundary conditions for flow and temperature fields at the aperture plane for two dimensional open-ended structures was obtained for a wide range of pertinent parameters such as Rayleigh number, Prandtl number, and aspect ratio by Khanafer and Vafai<sup>6</sup>.

Comprehensive comparisons for the streamlines and the isotherms within the enclosure were presented for various controlling parameters between the two-dimensional closed ended model (based on the use of effective boundary conditions) and the fully extended domain utilizing the far field boundary conditions.

Good agreement may be obtained between the numerical results and the corresponding experimental data in pressure and velocity distribution inside and around a scale cubic building model<sup>7</sup>, by applying large eddy simulation (LES) methodology to wind driven ventilation. Natural convection in open-ended cavities has received considerable attention by many researchers both experimentally and numerically. For thermal natural convection, the distribution of the total heat fluxes conveyed by the fluid flow through the open boundaries not only depends on heat transfer at walls but also on physical conditions prevailing in the surroundings, on both sides of the apertures<sup>8,9</sup>.

Effect of surrounding conditions on natural convection flow in a three dimensional cavity enclosed with another cavity equally distanced from the inner cavity is studied here numerically. The flow is considered to be steady, incompressible, viscous and turbulent. The  $k - \varepsilon$  turbulence model is used for simulation to capture the turbulent nature of the flow. Effects of surrounding temperature, opening positions etc. are studied and reported. Comparison of the present results with a previous work is also presented here to validate the model. Finally, a relation among the Nusselt number and other non-dimensional parameters is also reported in this study.

Since heat is transferred from hot medium to cold medium, the surrounding conditions of open cavity have a significant effect on the heat transfer mechanism as well as on the fluid flow characteristics. It is challenging to consider the surrounding conditions in numerical computations because of its sensitivity to the boundary conditions of the surrounding surfaces. To the best of knowledge, no research

\* Author for correspondence. e-mail: raaz2015@yahoo.com

has been carried out so far to assess the effects of surrounding conditions on the open cavity flow behavior. The present study is motivated to explore the phenomena.

## II. Description of the Model and Grid Distribution

In this work, buoyancy-driven natural convection flow in a 3D open cavity is studied numerically. In particular, a cavity of dimension 0.5 m (length)  $\times$  0.5 m (width)  $\times$  1.0 m (height) is considered as the reference case in this study. Heat is imposed at the left wall and the right wall is kept at constant temperature of the cavity. Zero heat flux is used at all other walls. Outside this cavity, another cavity is considered to observe the effects of natural convection heat transfer in air flow. All the surfaces of this outer cavity are considered at equal distance (e.g. 1m) from all the walls of the inner cavity. A figure of the geometry considered in present computation is shown in Fig. 1.

Non-uniform structured mesh is generated using ICEM CFD<sup>10</sup>, in order to discretize the computational domain. The finest possible grid containing about 0.49 million and 0.46 million hexahedral elements are used in inner and outer cavity, respectively. A minimum spacing 1mm, stretching factor of 1.2 and 26 grids in the radial direction up to a certain distance are generated in the inner cavity. Denser grids are used near the inner cavity in all sides of the outer cavity to observe the effects of mass flow and temperature just outside the inner cavity.

## III. Numerical Method

Computational Fluid Dynamics (CFD), based on the numerical solution of the mathematical equations governing the complex physical mechanisms has gained lead during the last few years. Gan<sup>11, 12</sup> suggested that the larger computational domain should be used for accurate prediction of heat transfer and

Nomenclature:	
$u, v, w$	$X, Y, Z$ -components of velocity respectively [ $ms^{-1}$ ]
$x, y, z$	Cartesian coordinates [ $m$ ]
$\beta$	Thermal expansion coefficient [ $K^{-1}$ ]
$\mu$	Dynamic viscosity [ $Kg m^{-1}s^{-1}$ ]
$\mu_T$	Turbulence viscosity [ $Kg m^{-1}s^{-1}$ ]
$\nu$	Kinematic viscosity [ $m^2s^{-1}$ ]
$\rho$	Density of the fluid [ $Kg m^3$ ]
$\sigma_T$	Thermal diffusivity [ $m^2s^{-1}$ ]
$C_p$	Specific heat capacity [ $J Kg^{-1}K^{-1}$ ]
$Gr$	Grashof number [-]
$L$	Length [ $m$ ]
$W$	Width [ $m$ ]
$H$	Height [ $m$ ]
$P$	Pressure [ $Kg m^{-1}s^{-2}$ ]
$k$	Turbulent kinetic energy [ $m^2s^{-1}$ ]
$g$	Gravitational acceleration [ $ms^{-2}$ ]
$\mathcal{E}$	Dissipation rate
$Pr$	Prandtl number [-]
$Ra$	Rayleigh number [-]
$Nu$	Nusselt number [-]
$T^*$	$(T-T_c)/\Delta T$

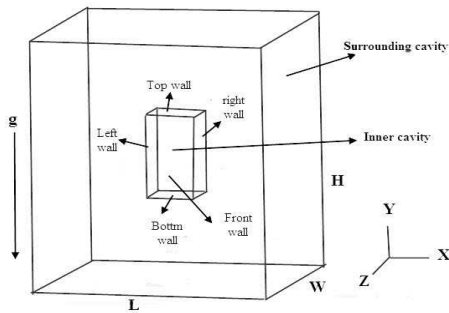


Fig. 1. Studied cavity with equally distant surrounding cavity

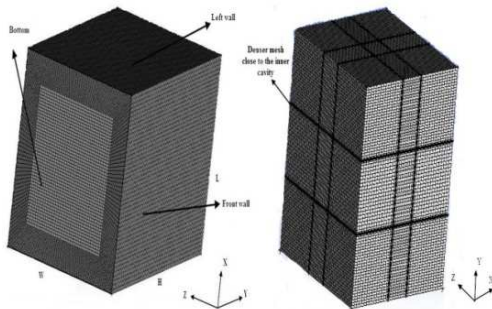


Fig. 2. Grid distribution on studied cavity (left) and equally distant surrounding cavity (right)

flow rate in ventilation cavities or enclosures with large openings. Two different models are considered, namely the two-equation  $k-\epsilon$  model and the Renormalization Group (RNG) theory for wind driven natural ventilation in a cubic building<sup>13</sup>.

ANSYS CFX-Solver Manager 12.0<sup>10</sup> is used to solve the governing equations at each grid of the sufficiently large computational domain. The convergent and grid independent solution with residual target  $10^{-4}$  is obtained using  $k-\epsilon$  turbulence model.

### Governing Equations and Boundary Condition

The flow in this study is considered to be steady, incompressible, three-dimensional, viscous, turbulent and buoyant. The Reynolds Averaged Navier Stokes (RANS) equations are as follows:

Continuity equation:

$$\frac{\partial}{\partial x_j}(u_j) = 0; j = 1, 2, 3; \quad (3.1)$$

Momentum equation

$$\rho u_j \frac{\partial}{\partial x_j} (u_i) = -\frac{\partial p}{\partial x_i} + \frac{\partial}{\partial x_j} [(\mu + \mu_T) \frac{\partial u_i}{\partial x_j}] + \rho_{ref} g_i \beta (T - T_{ref}); \quad i = 1, 2, 3; \quad j = 1, 2, 3; \quad (3.2)$$

$$\text{Energy equation: } u_j \frac{\partial}{\partial x_j} (T) =$$

$$\frac{\partial}{\partial x_j} \left[ \left( \frac{\nu}{Pr} + \frac{\nu_T}{\sigma_T} \right) \frac{\partial T}{\partial x_j} \right]; \quad j = 1, 2, 3; \quad (3.3)$$

According to the  $k-\varepsilon$  model,  $\mu_T$  can be expressed as follows:

$$\mu_T = C_\mu \rho \frac{k^2}{\varepsilon} \quad (3.4)$$

The  $k-\varepsilon$  model is the most widely known and extensively used two-equation eddy viscosity model. This model is sometimes referred as the standard  $k-\varepsilon$  model. The  $k$  equation is a model of the transport equation for the turbulent kinetic energy, and the  $\varepsilon$  equation is a model for the dissipation rate of turbulent kinetic energy. It is the simplest kind of model that permits prediction of both near-wall and free-shear-flow phenomena without adjustments to constants or functions. It successfully accounts for many low Reynolds number features of turbulence and its use has led to accurate predictions of flows with recirculation as well as those of the boundary layer kind<sup>14</sup>.

According to this model,  $k$  and  $\varepsilon$  can be obtained from the following equations:

$$\frac{\partial}{\partial x_j} (\rho u_j k) = \frac{\partial}{\partial x_j} \left[ \left( \mu + \frac{\mu_T}{\sigma_k} \right) \frac{\partial k}{\partial x_j} \right] + P_k - \rho \varepsilon \quad j = 1, 2, 3; \quad (3.5)$$

$$\frac{\partial}{\partial x_j} (\rho u_j \varepsilon) = \frac{\partial}{\partial x_j} \left[ \left( \mu + \frac{\mu_T}{\sigma_\varepsilon} \right) \frac{\partial \varepsilon}{\partial x_j} \right] + C_1 \frac{\varepsilon}{k} P_k - C_2 \rho \frac{\varepsilon^2}{k} \quad j = 1, 2, 3; \quad (3.6)$$

Here  $P_k$  is the production rate of turbulent kinetic energy which depends on the turbulent viscosity and velocity distribution. The values of all the empirical constants used in previous equations are presented in Table 1.

**Table 1. Empirical constants used in  $k-\varepsilon$  model**

$C_\mu$	0.09
$C_1$	1.44
$C_2$	1.92
$\sigma_k$	1.0
$\sigma_\varepsilon$	1.3

#### IV. Validation of Methodology

In any specific CFD approach the necessity of the surrounding domain, the proper turbulence model and the boundary conditions are the primary issues for computing the pure buoyancy driven flow phenomenon in the open cavity. Comparison with the study of Barakos et al.<sup>15</sup> for a closed cavity is given below to verify the numerical method.

*Comparison with the result reported by Barakos et al.<sup>15</sup>:*

Barakos et al.<sup>15</sup> studied the buoyancy driven laminar and turbulent air flow in a two dimensional closed cavity. The horizontal walls of the cavity were assumed to be perfectly adiabatic ( $\dot{q} = 0$ ). The vertical walls were kept isothermal with the left wall at high temperature  $T_H$  and the right wall at low temperature  $T_C$ . The interior of the cavity was filled with air and all properties are calculated at a reference temperature 293 K. Temperature difference of 20 K was kept between the vertical walls. Different Rayleigh numbers from  $10^3$  to  $10^{10}$  were considered to study. Temperature distribution with the present work for  $k-\varepsilon$  solution and Rayleigh number  $10^8$  is presented in Fig. 3. Some discrepancy is observed because the cavity considered in the Barakos's study was two dimensional. Hence the discrepancy with present study is probably due to 3D effect, discretization error and / or lack of sufficient convergence.

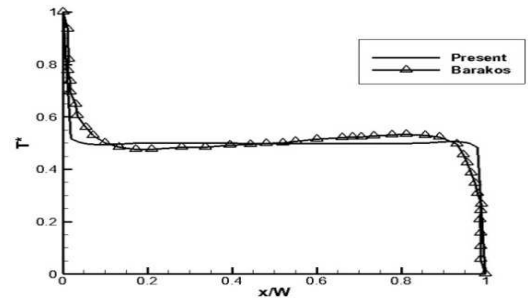


**Fig. 3.** Comparison of temperature distribution at mid length of the cavity ( $k-\varepsilon$ ) solution

#### V. Results and Discussion

Buoyancy driven natural convection flow in a three dimensional open cavity is studied here numerically. Choosing the perfect surrounding conditions, is an important task to understand the flow phenomena inside and outside the cavity clearly.

*Choosing an Extended Computational Domain*

It is necessary to assume an extended computational domain around the cavity to capture the heat transfer characteristics accurately<sup>10,11</sup>. The size of this computational domain has dominant effect on mass flow, temperature, velocity profile etc. In this study surroundings are chosen at 1m distance from every nearest parallel walls of the inner cavity. Average mass flow and temperature are observed by

considering the outer cavity at different distance (0.05m–1.4m) from the inner cavity. The results for 0.9m to 1.4m are shown in Table 2. From this numerical study it is observed that from 0.9m to 1.25m distant domain, difference in bottom average mass flow rate with 1m surrounding is less than 2%. Hence the difference in average temperature at bottom wall is negligible here. It is noted that variation in temperature and velocity profiles at different heights in the innercavity for these cases is also negligible(Fig. 4, 5).

Since the change in mass flow rate, temperature and velocity profile is negligible around 1m extended computational domain, it is chosen as reference case in this study.

*Effects of Opening Positions at Surrounding Boundaries*

In the reference case, the top and bottom walls of the surrounding cavity are considered to be open. In this section, the effects of different opening position in surrounding cavity are studied. The opening position at surrounding cavity has significant effect on the velocity profile inside the

inner cavity. Since the difference in temperature profile is not dominant in all cases. These results are not shown for brevity.

Average mass flow rate changes with the change of opening positions. Difference in mass flow rate, is the highest in case of all opening walls. At the bottom wall of the inner cavity, mass flow rate changes up to about 20% from bottom-top wall opening case (Table 3).

Opening position in surrounding cavity also affects the flow pattern inside the inner cavity (Fig. 6). It is observed that the flow pattern inside the inner cavity is more complex in case of bottom-top and front- rear opening than in other cases.

*Effects of Surrounding Temperature*

In this study the surrounding temperature is hitherto (till now) kept at 25°C. Two different surrounding temperatures 30°C and 35°C are assumed in this section and the comparison is made after comparing

**Table 2. Mass flow and temperature for different domain size**

Surround distance (m)	Mass flow rate (bottom) (Kg/s) × 10 <sup>-6</sup>	Mass flow rate (Top) (Kg/s) × 10 <sup>-6</sup>	Error (%) × 10 <sup>-3</sup>	Error in bottom mass flow rate with 1m (%)	Temperature (Bottom) (K)	Temperature (Top) (K)	Error (%)	Error in bottom temperature with 1m (%)
0.9	4.56356	-4.56356	0	1.54852	298.494	301.471	0.997	0.00134
1.0	4.49397	-4.49398	0.223	-	298.49	301.476	1.000	-
1.1	4.56432	-4.56424	1.753	1.56543	298.49	301.452	0.992	0.80375
1.25	4.57538	-4.57538	0	1.81154	298.488	301.437	0.988	1.23845
1.4	4.63380	-4.63380	0	3.11150	298.487	301.402	0.977	2.37678

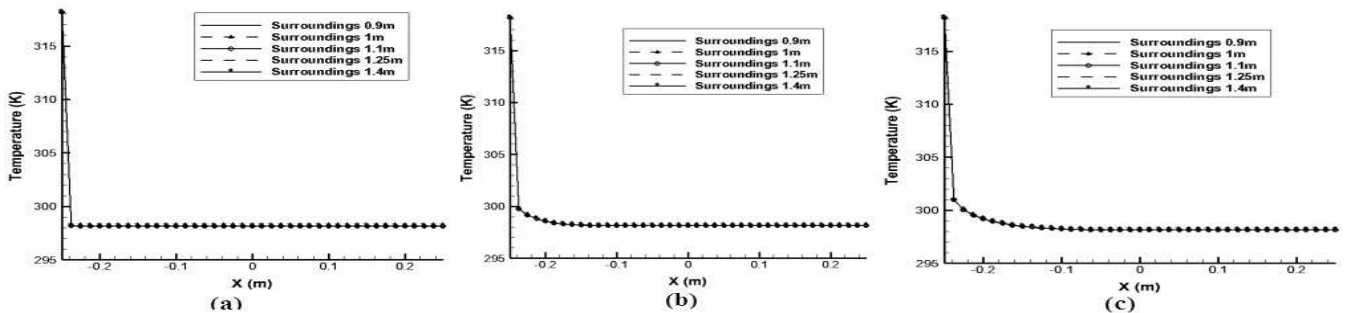


**Fig. 4.** Temperature profile (a): at y= -0.5 m (b): at y=0 m and (c): at y=0.5 m for different surroundings.

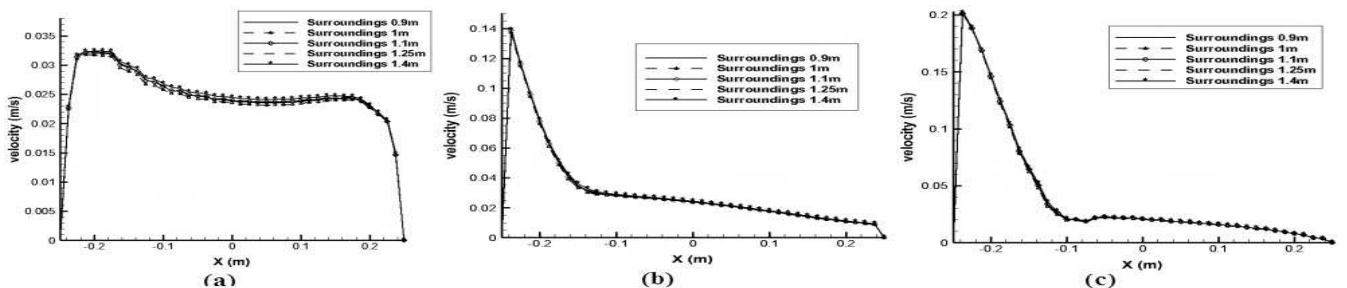


**Fig. 5.** Velocity profile (a): at y=-0.5 m (b): at y=0 m and (c): at y=0.5 m for different surroundings.

with the results of the reference case. Huge difference is observed between these cases. In both cases, the temperature and velocity profiles (Fig. 7) behave totally different than the case of surrounding temperature 25°C. The temperature inside the inner cavity becomes almost equal to the surrounding temperature, which is not shown for brevity. Mass flow rate at the bottom wall of the inner cavity and heat flux at the hot wall decrease with the increase of surrounding temperature. With only 5°C increase of surrounding temperature (25°C to 30°C), the stream-lines (Fig. 8b) adjacent to the side walls have become straight line. Turbulent nature is observed at the middle of the inner cavity. This behavior can be explained by the velocity vector (Fig. 8a). A downward flow is observed adjacent to

the cold wall and the velocity of the flow increases at the bottom wall which was not observed in case of surrounding temperature 25°C. It is because in case of surrounding temperature 25°C, the cold wall and surroundings have same temperature. But in case of surrounding temperature 30°C and 35°C, the cold wall temperature is less than the surrounding temperature. And the density of the air flow inside the cavity is greater than the density of the air flow outside the cavity. So a downward flow adjacent to the cold wall is observed due to buoyancy force. A downward flow has arisen adjacent to the cold wall (Fig. 9) in case of surrounding temperature 30°C and 35°C which is absent in case of 25°C. The streamlines outside the inner cavity show laminar flow for surrounding temperature 25°C.

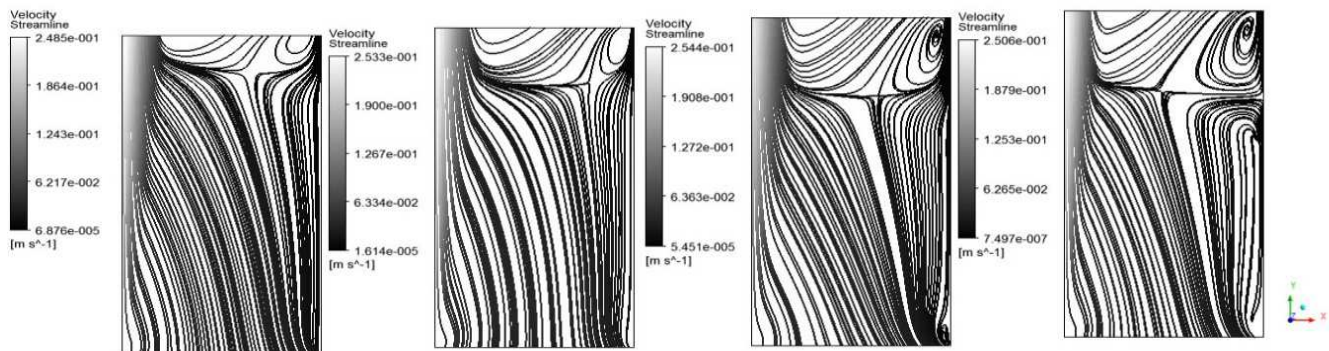


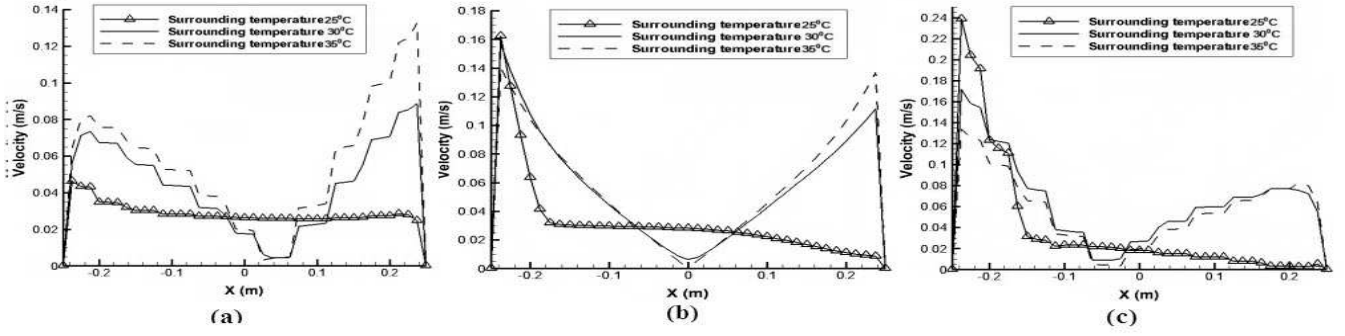
Fig. 6. Streamlines on a vertical plane at mid width of the inner cavity (bottom-top, front-rear, left-right and all opening walls of surrounding cavity are open respectively).

Table 3. Average mass flow and heat flux for different opening position

Opening position	Mass flow rate (bottom) (Kg/s) $\times 10^{-6}$	Mass flow rate (top) (Kg/s) $\times 10^{-6}$	Error with reference case (%)	Average heat flux (left) W/m <sup>2</sup>	Error with reference case (%)
Bottom and top walls	1.2512	-1.25117	-	32.6543	-
Front and rear walls	1.19075	-1.19075	5.20085	33.828	3.59585
Left and right walls	1.16231	-1.16233	7.10438	33.7352	3.31013
All walls	0.99528	-0.99529	20.45364	33.2519	1.83008

Table 4. Mass flow, temperature and heat flux for different surrounding temperature

Surrounding Temperature (°C)	Mass flow rate (bottom) (Kg/s) $\times 10^{-6}$	Mass flow rate (top) (Kg/s) $\times 10^{-6}$	Bottom temperature (K)	Top Temperature (K)	Average heat flux (left wall) W/m <sup>2</sup>
25	1.2512	-1.25117	298.162	300.244	32.654
30	0.350632	-0.350635	304.273	308.49	25.1
35	-0.026614	0.026611	267.816	267.941	15.46



**Fig. 7.** Velocity profile (a): at  $y = -0.5$  m (bottom) (b): at  $y = 0.0$  m (middle) (c): at  $y = 0.5$  m (top) of the inner cavity along X-axis for different surrounding temperature.

But the streamlines for surrounding temperatures 30°C and 35°C are no more laminar at the top and bottom openings. Therefore, it can be concluded that the surrounding temperature is one of the most important conditions in the study of natural convection flow in open cavity.

#### Some Non-dimensional Parameters

Mass flow and heat transfer are the main concerns in the buoyancy driven natural convection flow. Non-dimensional parameters are important to understand the physics of the model. A relation between Nusselt Number, Rayleigh number and Prandtl number was reported by Bejan<sup>16</sup>. This relation is proposed for a hot vertical wall with high Rayleigh number and low Prandtl number as follows:

$$Nu_h = \frac{h_{0-H}H}{k} \cong 0.19Ra_H^{1/3} Pr^{1/3} \quad (Pr \ll 1) \quad (5.1)$$

In this expression,  $h_{0-H}$  is the heat transfer coefficient averaged over the wall height  $H$  and  $Ra_H$  is the Rayleigh number based on  $H$  and  $(T_0 - T_\infty)$ .

$$Ra_H = \frac{g\beta\Delta TH^3 Pr}{\nu^2} \quad (5.2)$$

The expression (5.1) is applicable for all temperature difference and heat flux. The coefficient 0.19 is replaced by 0.198 if the wall condition is of uniform heat flux<sup>16</sup>. In the present study, this relation (Eq. 5.1) is found to be as follows:

$$Nu_H = \frac{h_{0-H}H}{k} \cong 0.15(Ra_b Pr)^{1/3} \quad (Pr \ll 1) \quad (5.3)$$

where Rayleigh number  $Ra_b$  is based on the cavity width  $b$  and defined as:

$$Ra_b = \frac{g\beta\Delta T b^3 Pr}{\nu^2} \quad (5.4)$$

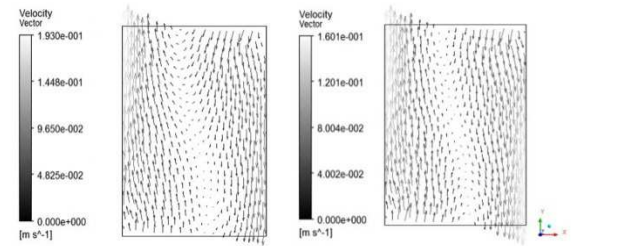


**Fig. 8 (a).** Velocity vectors on a vertical plane at mid width of the inner cavity for Surrounding temperature 30°C (left) and 35°C (right).

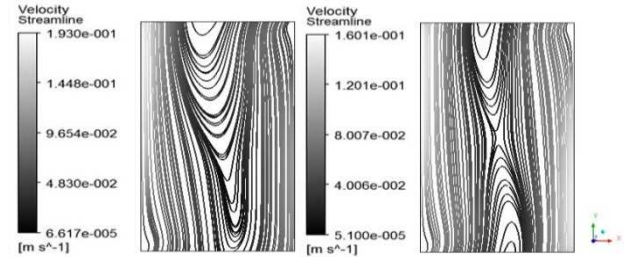


**Fig. 8 (b).** Streamlines on a vertical plane at mid width of the inner cavity for Surrounding temperature 30°C (left) and 35°C (right).

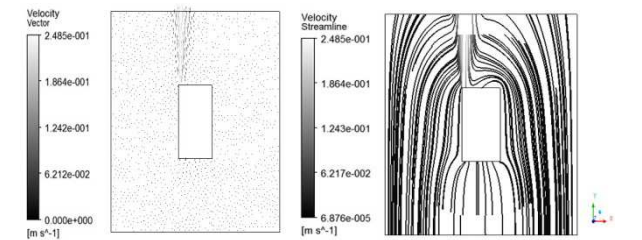


**Fig. 9 (a).** Velocity vector (left) and stream line (right) at mid width of the outer cavity for surrounding temperature 25°C.

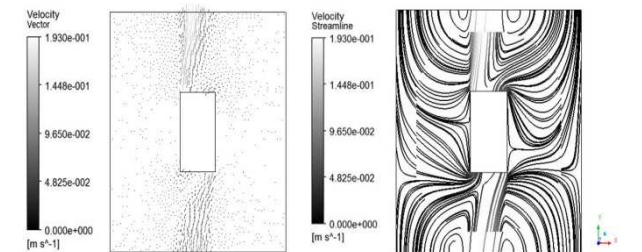


**Fig. 9 (b).** Velocity vector (left) and stream line (right) at mid width of the outer cavity for surrounding temperature 30°C.

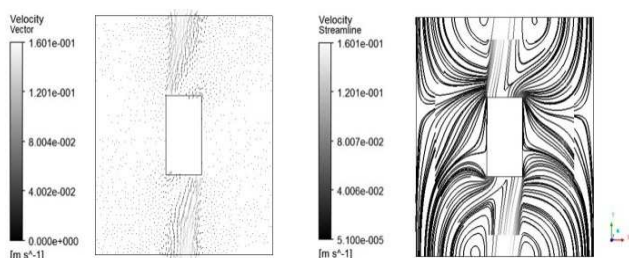


**Fig. 9 (c).** Velocity vector (left) and stream line (right) at mid width of the outer cavity for surrounding temperature 35°C. Prandtl number is defined as:

$$Pr = \frac{\mu C_p}{k} \quad (5.5)$$

Nusselt number  $Nu_H$  is calculated based on the cavity height  $H$ . Fig. 10 shows the Nusselt number for different  $Ra$  number (Eq. 5.3).

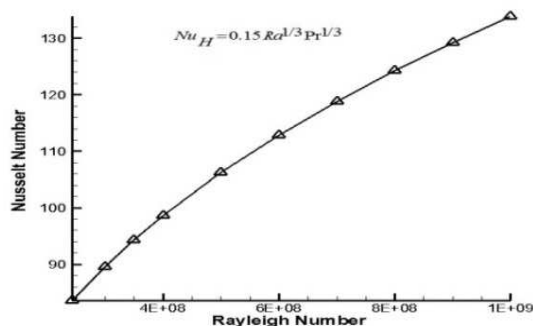


**Fig. 10.** Relation between Nusselt number and Rayleigh number (Eqn. 5.3)

## VI. Conclusions

The effects of boundary conditions at the surfaces of the extended computational domain in computing the natural convection flow in a three dimensional open cavity are studied numerically. Since buoyancy is the dominant heat transfer mechanism, surrounding boundary conditions have a sensitive effect on the flow inside the cavity. The solution captures all flow and heat transfer phenomena well, especially near the wall where dense and finest grids are used. Good agreement is found with previous work.

A sufficiently large extended computational domain is ensured to capture the flow phenomena accurately. It is observed that the change in flow and heat transfer characteristics inside the cavity occurs due to the effects of different surrounding boundary conditions. Velocity and temperature adjacent to the hot and cold walls are found to be changing more than the other locations inside the cavity for all conditions. Significant change in mass flow, velocity and temperature is observed by changing the surrounding temperature slightly. Opening positions on the outer cavity also has significant effects on the mass flow and turbulent nature of the flow inside the cavity. A relation between the non-dimensional parameters is found as  $Nu \cong 0.15(Ra_b Pr)^{1/3}$  that may be applied to understand physical mechanism.

## References

1. Agrawal Nilesh, Seik Mansoor Ali, K. Velusamy, S.K. Das, 2010. Numerical study of natural convection in an enclosure with and without Boussinesq assumption - A comparative study, Proceedings of the 37th National & 4th International Conference on Fluid Mechanics and Fluid Power, December 16-18, IIT Madras, Chennai, India.
2. Bangalee, M.Z.I., J.J. Miao, S.Y. Lin, 2013. Computational techniques and a numerical study of a buoyancy-driven ventilation system, International Journal of Heat and Mass Transfer **65**, 572–583.
3. Bejan, A. S. Kimura, 1981. Penetration of free convection into a lateral cavity, J. Fluid Mechanics **103**, 465–478.
4. Fusegi, T., J.M. Hyun, K. Kuwahara and B. Farouk, 1991. A numerical study of three-dimensional natural convection in a differentially heated cubical enclosure, Int. J. Heat Mass Transfer **34**, 1543-1557.
5. Fusegi, T., J.M. Hyun and K. Kuwahara, 1991. Three-dimensional simulations of natural convection in a sidewall-heated cube, International Journal of numerical Methods of Fluids **3**, 857-867.
6. Khanafer, K., K. Vafai, 2002. Effective boundary conditions for buoyancy-driven flows and heat transfer in fully open-ended two-dimensional enclosures, International Journal of Heat and Mass Transfer **45**, 2527–2538, 2001.
7. Jiang, Y., D. Alexander, H. Jenkins, R. Arthur, Q. Chen, 2003. Natural ventilation in buildings: measurements in a wind tunnel and numerical simulation with large-eddy simulation, Journal of Wind Engineering and Industrial Aerodynamics **91**, 331–353.
8. Sun, H., R. Li, E. Chénier, G. Lauriat, 2012. On the modeling of aiding mixed convection in vertical channels, Heat Mass Transfer 1–10.
9. Aihara, T., 1973. Effects of inlet boundary conditions on numerical solutions of free convection between vertical parallel plates, Report of the Institute of High Speed Mechanics, Tohoku University, Japan **28**, 1–27.
10. ANSYS 12.0, Ansys Inc., User manual.
11. Gan Guohui, 2010. Simulation of buoyancy-driven natural ventilation of buildings-Impact of computational domain, Energy and Buildings **42**, 1290–1300.
12. Gan Guohui, 2010. Impact of computational domain on the prediction of buoyancy-driven ventilation cooling” Building and Environment **45**, 1173–1183.
13. Evola, C., V. Popov, 2006. Computational analysis of wind driven natural ventilation in buildings, Energy and Buildings **38**, 491–501.
14. Launder, B. E., D. B. Spalding, 1974. The Numerical Computation of Turbulent Flows, Computer Methods in Applied Mechanics and Engineering **3**, 269-289.
15. Barakos, G., E. Mitsoulis and D. Assimacopoulos, 1994. Natural Convection Flow in A Square Cavity Revisited: Laminar and Turbulent Models with Wall Functions, International Journal for Numerical Methods in Fluids **18**, 695-719.
16. Bejan, A., Convection Heat Transfer, Fourth Edition, John Wiley & Sons, Durham, North Carolina.